Hindawi
Journal of Nanomaterials
Volume 2017, Article ID 5658796, 12 pages
https://doi.org/10.1155/2017/5658796

Research Article

One-Electron Conical Nanotube in External Electric and Magnetic Fields

L. F. Garcia, W. Gutiérrez, and I. D. Mikhailov

Universidad Industrial de Santander, A. A. 678, Bucaramanga, Colombia

Correspondence should be addressed to L. F. Garcia; lfraqgar@gmail.com

Received 11 August 2016; Accepted 23 January 2017; Published 15 February 2017

Academic Editor: Xin Zhang

The effects of variation of the aperture angle on spectral and magnetic properties of one-electron nanotube of the axially symmetrical conical shape in the presence of the electric and magnetic fields have been investigated based on a numerical solution of the Schrödinger equation in the effective mass approximation. We show that the energy spectrum and the magnetic dipole moment of the structure are changed dramatically with increase of the cone's aperture angle due to the interplay between the diamagnetic and centrifugal forces, which push the electron at opposite directions. Particularly, the energy levels close to the ground state become quasi-degenerate, owing to a change of the hidden symmetry, induced by the magnetic field in this structure, when its morphology is converted from the cylindrical type to the conical one and the Aharonov-Bohm oscillations of the ground state energy and of the magnetic dipole moment are quenched. We found additionally that any weak electric field breaks this hidden symmetry, splits quasi-degenerate state, and restores the Aharonov-Bohm oscillations.

1. Introduction

One-dimensional nanostructures such as wires and tubes are object of intensive research at last decade owing to their unique applications in fabrication of nanoscale devices [1–3]. They are expected to play an important role as functional units in fabricating of optoelectronic devices with nanoscale dimensions. One of their applications is related to solar cells based on new photovoltaic technologies. As it has been recently demonstrated a very promising way to this goal gives a hybrid solar cell covered in silicon nanocones and a conductive organic polymer [4–6]. Another possible interesting route for one-dimensional nanostructure applications is designing of nanoantennas as solid-state single photon sources [7]. A strong dependence of the absorption of light on the geometry has been revealed recently by comparing the properties of the cylindrical and conical nanowires [8]. For optical properties of the wires, related to absorption and emission of the light, an important parameter is their polarizability, mainly governed by the anisotropic quantum confinement, but it also can be controlled by external electric and magnetic fields.

An important particularity of one-dimensional structures with axial symmetry is their extraordinary sensibility to external magnetic field related to the Aharonov-Bohm (AB) effect. Previously, AB effect has been studied for narrow quantum rings (QRs) with one and two electrons [9, 10] and with neutral and charged excitons [11–16].

It was shown previously that the presence of any nonuniformity [17–19] or an impurity [20] in a circular QR generates a partition of the closed paths of particles and quenching of the AB oscillations of one- and two-particle energy levels. One can expect that the similar magnetic properties but with weaker sensibility to defects could have narrow nanotubes where, unlike the QR, there are an infinite number of closed paths over the cylindrical surface that do not pass through defect location. AB oscillations in photoluminescence from charged exciton in InAs tubes with a thickness of several monolayers have been experimentally revealed recently [21].

Another source of a delicate nature of the AB effect in wide QRs is the spatial separation of closed classical paths corresponding to states with different angular momenta in the presence of the external magnetic field. The higher the magnetic field, the stronger is the separation between these paths and the weaker is the interference of the corresponding wave functions responsible for the AB effect. As a consequence, the amplitude of the AB oscillation is significant only

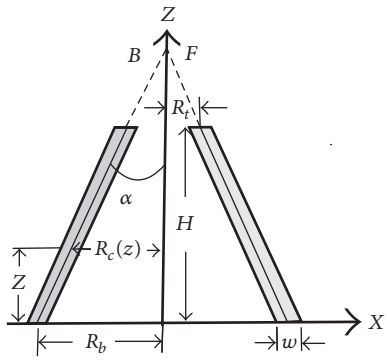

Figure 1: Vertical cross-section of conical nanotube.

if the ring is sufficiently narrow. On the other hand, in the limiting case of 1D ring the dephasing due to defects becomes such strong that it can suppress these oscillations completely. Therefore, a thin quantum tube could be a good alternative for observing the AB effect of one- and two-particle composite systems confined in them [21].

Recently, it has been demonstrated that microtube structures can be fabricated by using lattice-mismatched epitaxial layers that rolled up when freed from the substrate due to the built-in strain [22]. We believe that this technique also offers an opportunity to design nanotubes with variable cross-section radii, in which the spatial separation of the classical paths corresponding to the states with different angular momentum may be controlled by means of external fields. In order to check such possibility, we study in this paper the spectral properties of one-electron thin nanotube of the conical form with different aperture angles in the presence of external magnetic and electric fields applied simultaneously along the symmetry axis.

The paper is organized as follows. In the next section we consider a model of a thin one-electron nanotube of a conical form and describe the procedure of the separation of variables in the framework of the adiabatic approximation. The numerical results and the analysis of energies dependencies on the magnetic field in the zero-electric-field case are presented in Section 3. Also here we analyze similar dependencies for the magnetic dipole moment. The influence of the electric field on the AB oscillation and the nanotubes magnetic dipole moment is considered in Section 4. Finally, some conclusions are presented in Section 5.

2. Theoretical Model

We consider a model of a nanotube of conical form with the geometrical parameters: the height H, the thickness w, the aperture angle α, and the bottom and the top radii R_b and R_t, respectively (se Figure 1). The aperture angle α is related to dimensions of the nanotube as

$$\tan\alpha = \frac{(R_b - R_t)}{H}. \tag{1}$$

Horizontal cross-sections of the structure are QRs of unchanged thickness w and with different centre-line radii which depend on the coordinate z:

$$R_c(z) = R_b - z\tan\alpha = R_b \cdot \left(1 - \frac{z}{H}\right) + R_t \cdot \frac{z}{H}. \tag{2}$$

The following relations define in cylindrical coordinates (r, φ, z) the interior nanotube region frontiers:

$$0 < z < H; \quad R_c(z) - \frac{w}{2} < r < R_c(z) + \frac{w}{2}. \tag{3}$$

In our model, the external, magnetic B and electrical F fields are parallel to the z-axis. We use the effective Bohr radius $a_0^* = \hbar^2\varepsilon/m^*e^2$, the Rydberg $R_y^* = e^2/2\varepsilon a_0^*$, and the parameters $\xi = eFa_0^*/R_y^*$ and $\gamma = e\hbar B/2m^*cR_y^*$ as units of length, energy, and the dimensionless electric and magnetic fields, respectively. In what follows, we use the material parameters typical for thin GaAs layers, in which the corresponding scales are $a_0^* \approx 10$ nm and $R_y^* \simeq 5$ meV [20]. We adopt a simple model with the infinite-barrier confinement, in which the potential is supposed to be equal to zero inside the nanotube region (3) and to infinity otherwise. The variable φ can be separated due to the axial symmetry of the structure, and with m being the Z-projection of the angular momentum, the corresponding wave function $\Psi_m(r, \varphi, z) = e^{im\varphi}\psi_m(r, z)$, $m = 0, \pm1, \pm2, \ldots$, satisfies the following wave equation:

$$\left[-\Delta_{r,z} + \left(\frac{m}{r} - \frac{\gamma r}{2}\right)^2 + \xi \cdot z\right]\psi_m(r, z) = E\psi_m(r, z); \quad 0 < z < H;\ R_c(z) - \frac{w}{2} < r < R_c(z) + \frac{w}{2}. \tag{4}$$

Here $\Delta_{r,z}$ is the part of the Laplace operator in polar coordinates that includes only radial and axial terms.

Below we consider only a case of very thin nanotube ($w \ll R_t$), taking into account the fact that thicknesses of experimentally fabricated tubes have the essentially smaller than their radii [20]. Moreover, this condition allows us to find solutions of (4) corresponding to the lower energies taking advantage of the adiabatic approximation. Indeed, the confinement within a thin and long nanotube with infinite-barrier confinement is strongly anisotropic, the coordinates $\tilde{r} = r - R_c(z)$ and z in a thin nanotube are restricted within a rectangular region of the very narrow thickness w and very high height H, and therefore the electron motion in the r direction is essentially faster than one in the z direction.

Following the well-known two-step adiabatic procedure, we represent the solution of (4) in the form $\psi_m(r, z) = \phi_m(\tilde{r}, z) f(z)$, where the first and the second factors describe, respectively, the rapid electron motion at the radial direction and the slow along the symmetry axis. The procedure is performed of first finding of the lowest eigenvalue $\tilde{E}_m^{(r)}(z)$ of the equation:

$$\left[-\frac{1}{\tilde{r}}\frac{d}{d\tilde{r}}\tilde{r}\frac{d}{d\tilde{r}} + \left(\frac{m}{r} - \frac{\gamma r}{2}\right)^2 - \tilde{E}_m^{(r)}(z)\right]\phi_m(\tilde{r}, z) = 0 \quad r = R_c(z) + \tilde{r};\ -\frac{w}{2} < \tilde{r} < +\frac{w}{2}; \tag{5}$$

$$\phi_m\left(-\frac{w}{2}, z\right) = \phi_m\left(+\frac{w}{2}, z\right) = 0.$$

Here the variable z is treated as parameter (*cf.* electronic motion for fixed nuclear position in molecular problem). Once the problem (5) is solved and the lowest energy $\widetilde{E}_m^{(r)}(z)$ is found, then

$$-\frac{d^2 f_n(z)}{dz^2} + U_m(z) f_n(z) = E_{m,n} f_n(z);$$
$$U_m(z) = \xi \cdot z + \widetilde{E}_m^{(r)}(z);\ R_t \cot\alpha < z < R_b \cot\alpha; \quad (6)$$
$$f_n(R_t \cot\alpha) = f_n(R_b \cot\alpha) = 0;$$
$$n = 1, 2, 3, \ldots.$$

The function $U_m(z)$ governs the vertical displacement of the plane of the electron rotation around the z-axis, and in what follows we call it the adiabatic potential.

One can find this function by solving the eigenvalue problem (5) for different values of the parameter z. The analytical solution of this problem has a form of a linear combination of hypergeometric functions and correspondent eigenenergies $\widetilde{E}_m^{(r)}(z)$ are the roots of a transcendental equation. However, for the case of a very thin nanotube, one can find simple expressions for $\widetilde{E}_m^{(r)}(z)$ and $\widetilde{U}_m(z) = U_m(z) - j_{0,1}^2/w^2$ in the first order of the perturbation theory, considering the ratio $w/R_c(z)$ as a small parameter:

$$\widetilde{U}_m(z) \approx \begin{cases} \xi \cdot z + \left[\dfrac{m}{R_c(z)} - \dfrac{\gamma \cdot R_c(z)}{2}\right]^2; & z \in (0, H) \\ \infty; & z \notin (0, H). \end{cases} \quad (7)$$

Here $j_{0,1} = 2.4048$ is the first root of the Bessel function $J_0(x)$. In our numerical work, we solve (6) with the adiabatic potential (7) by using the numerical trigonometric sweep method [23] and we find electron energies $E_{m,n}$ for twenty different magnetic quantum numbers $m = 0, -1, -2, \ldots, -19$ and two different axial quantum numbers $n = 1, 2$. Below, we present results of calculations for the conical nanotube with geometrical parameters, the base radius $R_b = 6a_0^*$, the height $H = 20a_0^*$, the thickness $w = 0.2a_0^*$, and y different aperture angles from $\alpha = \arctan 0.25$ corresponding to the case of the cylindrical nanotube, corresponding to aperture angle $\alpha = 0$ and $R_t = 1a_0^*$ up to $\alpha = \arctan 0.25$ and $R_t = 1a_0^*$. In what follows we present the results for the renormalized electron energies defined as $\widetilde{E}_{m,n} = E_{m,n} - j_{0,1}^2/w^2$.

3. Zero-Electric-Field Case

Let us first analyze the vertical displacement of the position of the stationary point $z_{\min}$, corresponding to the minimum of the potential $\widetilde{U}_m(z)$, induced by the external magnetic field γ. The values of $z_{\min}$ and $\widetilde{U}_m(z_{\min})$ define the position of the plane of the classical horizontal circular track and the classical energy of the rotational state with the angular momentum m and the study of their evolution under external fields allows us to give below a simple interpretation of the spectral and magnetic and electric properties of the conical nanotube.

According to (7), the potential minimum position in the zero-electric-field case ($\xi = 0$) depends on interplay between the centrifugal force, which pushes the electron toward the cone bottom, and the magnetic confinement that drives it to the cone top. The potential minimum position is situated at the cone bottom ($z_{\min} = 0$) until the increasing magnetic field remains weak ($\gamma \prec \gamma_1 = 2m/R_b^2$), and $\widetilde{U}_m(z_{\min}) = (m/R_b - \gamma \cdot R_b/2)^2$ falls up to zero, when the magnetic field tends to its lower threshold γ_1. As γ increasing further surpasses γ_1, the minimum position $z_{\min} = \sqrt{2m/\gamma}$ is displaced from the cone's bottom toward the top until the magnetic field reaches the upper threshold ($\gamma_2 = 2m/R_t^2$) while the potential energy minimum maintains a zero value $\widetilde{U}_m(z_{\min}) = 0$. Finally, as the magnetic field increasing exceeds the upper threshold value ($\gamma \succ \gamma_2$), the potential minimum position continues staying at the cone top ($z_{\min} = R_t \cot\alpha$) while the corresponding energy $\widetilde{U}_m(z_{\min})$ begins to rise.

In Figure 2 we present the evolution of the minima of the adiabatic potentials for some lower states under increasing magnetic field in conical nanotubes with three different magnetic aperture angles. Arrows show trends of displacements of the corresponding minima positions in increasing magnetic field. It is seen that classical electron paths, associated with adiabatic potential minima, align in a sequence of horizontal circular tracks climbing under increasing magnetic field one by one in ascending order of the angular momentum, from the bottom of the cone toward its top. The number of tracks lifting at the same time between the bottom and the top of the nanotube depends on the magnetic field value; the larger the magnetic field is, the greater the number of such tracks is. All classical circular tracks that satisfy the condition $\gamma R_t^2/2 < m < \gamma R_b^2/2$ for given γ are located between the bottom and the top of the nanotube ($0 < z_{\min} < H$) at the altitude

$$z_{\min} = H \cdot \frac{\left(R_b - \sqrt{2m/\gamma}\right)}{(R_b - R_t)}; \quad \frac{2m}{R_b^2} < \gamma < \frac{2m}{R_t^2}. \quad (8)$$

The energies minima of these rotational states remain equal to zero during escalation. In Figure 3, we show as example the potential curves for the case $\gamma = 0.5$, $R_b = 6a_0^*$, $R_t = 4a_0^*$ for which quantum numbers $m = 4, 5, 6, 7, 8, 9$ satisfy conditions (8).

From Figure 3, one can see that the potential curves, positioned between the bottom and the top of the nanotube, have the almost parabolic shape and therefore in the harmonic approximation the following analytical expressions for energies can be found from (6), by using the power series expansion of the potential (7) about the point $z_{\min}$:

$$\widetilde{E}_{n,m} \approx \gamma(2n-1)\tan\alpha; \quad \frac{2m}{R_b^2} < \gamma < \frac{2m}{R_t^2}. \quad (9)$$

Formulae (8) and (9) show that the energy spectrum of the one-electron conical nanotube acquires in the presence of the axially directed external magnetic field two peculiar features. At first, energies of states with quantum numbers m between $\gamma R_t^2/2$ and $\gamma R_b^2/2$ in the harmonic approximation depend only on the external magnetic field and the cone

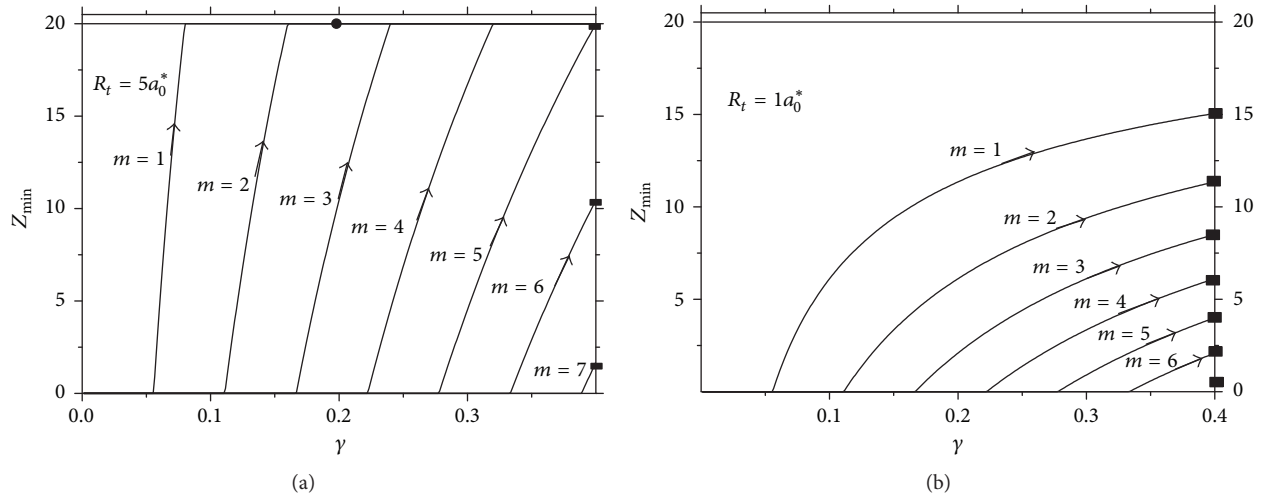

FIGURE 2: Escalation of the adiabatic potential minima positions along z-axis under increasing magnetic field for lower states in conical nanotube with dimensions $R_b = 6a_0^*$, $H = 20a_0^*$, and $w = 0.2a_0^*$, for two different top radii R_t.

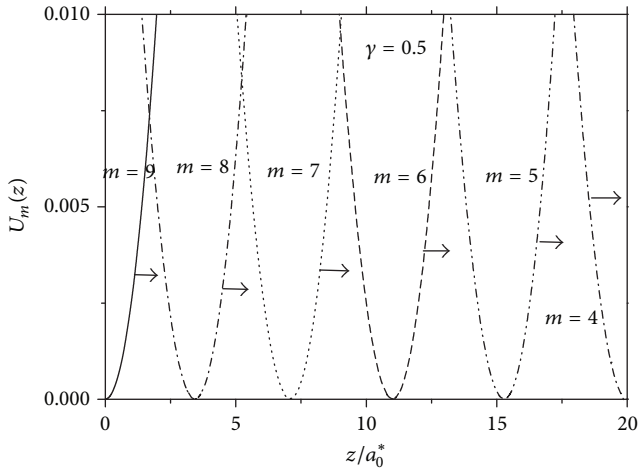

FIGURE 3: Adiabatic potential along z-axis for lower states and for the magnetic field. $\gamma = 0.5$. Arrows indicate directions of displacements of potential curves under increasing magnetic field.

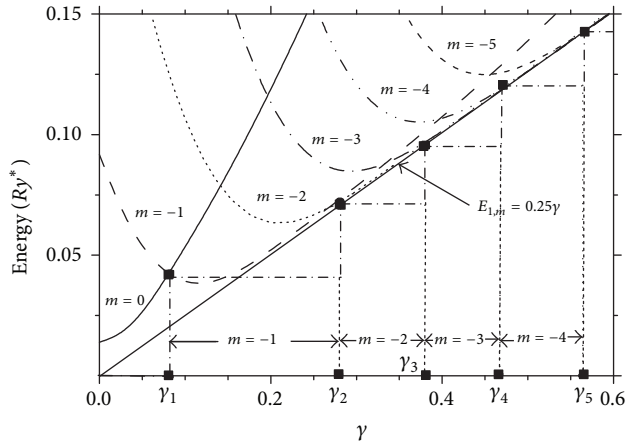

FIGURE 4: Six lower energies as functions of the external magnetic field in one-electron conical nanotube with dimensions $R_b = 6a_0^*$, $R_t = 1a_0^*$, $H = 20a_0^*$, and $w = 0.2a_0^*$. The dash-dot step-like line indicates the variation of the ground state angular momentum and symbols show the points of curves crossovers.

aperture angle, but they are independent on the angular momentum m. Therefore, there are $k > 1$ lower states ($k = \text{int}[\gamma(R_b^2 - R_t^2)/2]$) with different angular momenta, but with almost equal energies; that is, the lowest energy level is k-fold quasi-degenerate. On the contrary, the most probable electron positions along the tube axis in these states depend strongly on the angular momentum m according to the relation (8). Therefore, by increasing magnetic field applied along the nanotube axis one can create an arbitrary number of quasi-degenerate, spatially separated states with mutually orthogonal wave functions.

In Figure 4 we present results of calculation of six lower energies corresponding to the radial quantum number $n = 1$ as functions of the magnetic field in nanotubes with the aperture angle $\tan\alpha = 0.25$ and dimensions $R_b = 6a_0^*$, $R_t = 1a_0^*$, $H = 20a_0^*$. The straight line in Figure 4 has a slope in an excellent accordance with relation (9). Points of the crossovers between curves corresponding to the states with the angular momenta $m - 1$, m and correspondent values of the magnetic fields are marked by solid rectangular symbols. Starting from the crossover points γ_m, the energies grow linearly as functions of the magnetic field until the electron, rising along the z-axis, achieves to arrive up the cone top. The dash-dot polygons shown at the lower part of Figure 4 point out jumps of the ground state angular momentum at the points of the curves crossovers. It is seen that these jumps of the angular momentum are accompanied by the inversion of the energy levels and by a very weak splitting between them in a way that they become quasi-degenerate.

In Table 1, we present the energies of the seven lower energies for different values of the magnetic field calculated for a conical nanotube with the same dimensions in Figure 4,

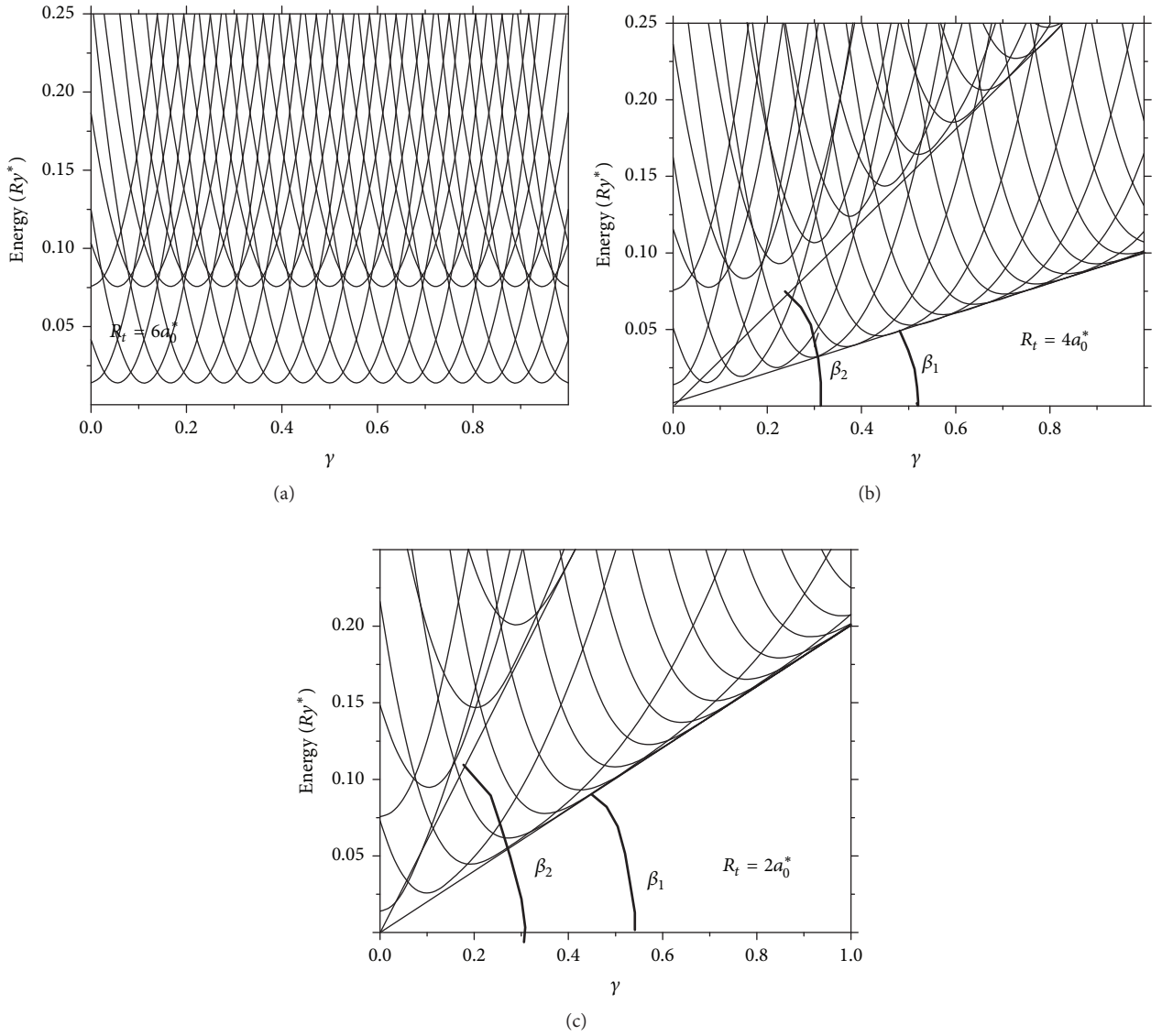

Figure 5: One-electron energies as functions of the external magnetic field in conical nanotubes with fixed dimensions $R_b = 6a_0^*$, $H = 20a_0^*$, and $w = 0.2a_0^*$ and for three different top radii R_t.

Table 1: Energies (given in Ry^* with error bars $0.005Ry^*$) of lower levels in one-electron conical nanotube with $R_b = 6a_0^*$, $R_t = 1a_0^*$, and $H = 20a_0^*$ and for different magnetic fields. Bold numbers indicate quasi-degenerate levels.

γ	m							
	0	1	2	3	4	5	6	7
.00	.01	.09	.25	.47	.76	1.1	1.5	1.9
.25	.16	**.07**	**.07**	.09	.15	.27	.44	.67
.50	.38	.14	**.13**	**.13**	**.13**	**.13**	.14	.19
.75	.66	.24	**.19**	**.19**	**.19**	**.19**	**.19**	**.19**
1.00	.98	.36	.26	**.25**	**.25**	**.25**	**.25**	**.25**
1.50	1.8	.72	.41	**.38**	**.38**	**.38**	**.38**	**.38**
1.75	2.2	.95	.50	**.44**	**.44**	**.44**	**.44**	**.44**

where bold numbers indicate quasi-degenerate levels. A consistent growth of number of quasi-degenerate states with the increase of the magnetic field is seen, which we ascribe to a change of the hidden symmetry, induced by the magnetic field in a structure, when its morphology is converted from the cylindrical type to the conical one.

In Figure 5, we present results of calculation of lower energies as functions of the magnetic field in nanotubes with the base radius $R_b = 6a_0^*$ and three different top radii R_t. Curves are shown for quantum numbers $n = 1, 2$ and $m = 0, 1, 2, \ldots, 15$. One can observe multiple crossovers of curves and a reordering of the energy levels, typical for AB effect observed for all aperture angles. Nevertheless, there is an essential modification of energies dependencies when the aperture angle is increased, primarily due to the rise of slopes of two envelope straight lines that mark off bands bottoms.

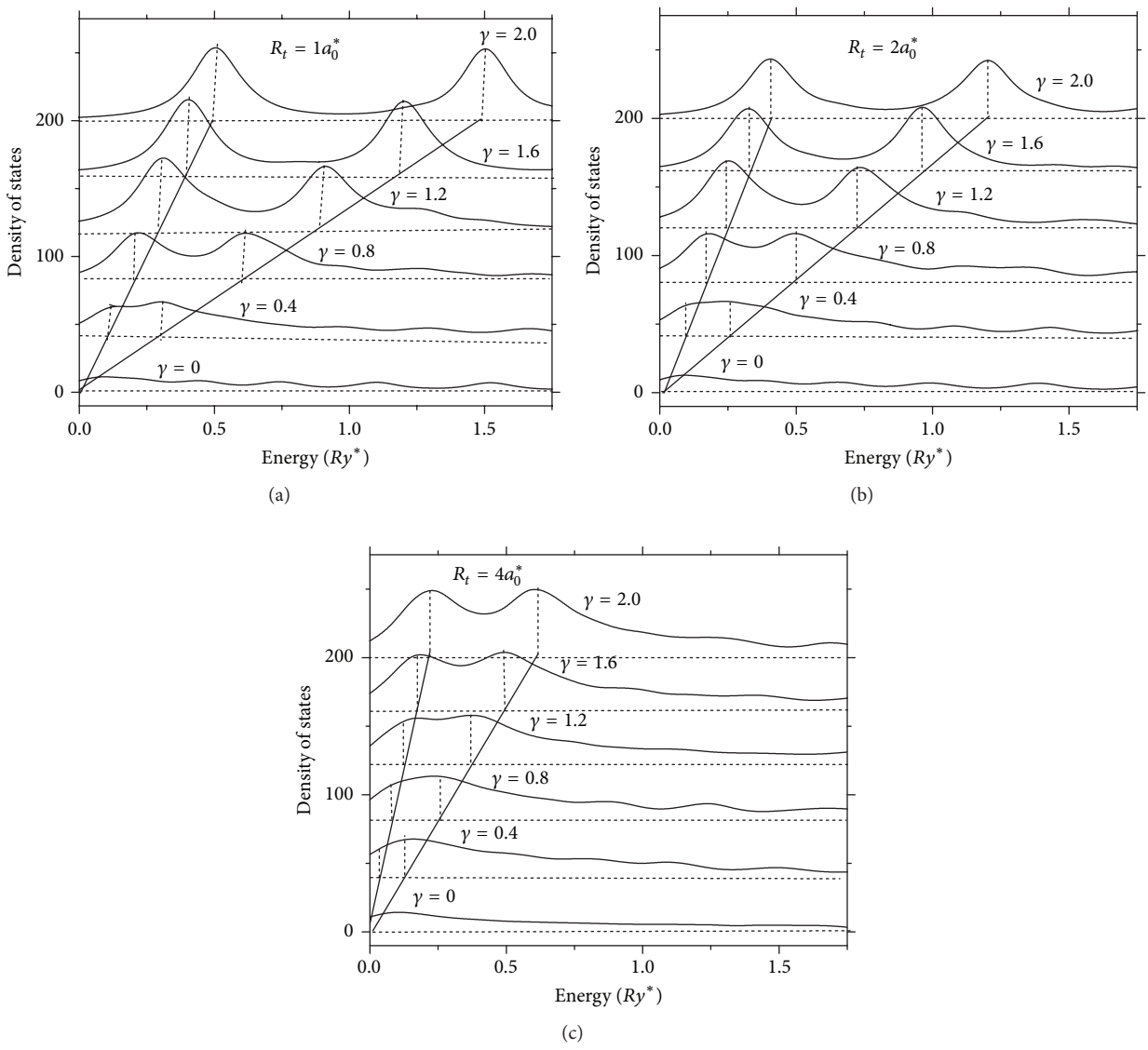

Figure 6: Density of states of one-electron conical nanotubes with fixed dimensions $R_b = 6a_0^*$, $H = 20a_0^*$, and $w = 0.2a_0^*$ for three different top radii R_t and different values of the external magnetic field.

At the case of the cylindrical nanotube, when the aperture angle is equal to zero, two overlapping bands in Figure 5(a) correspond to axial quantum numbers $n = 1, 2$.

Although energies dependencies on the field in the conical nanotubes with aperture angles different from zero in Figures 5(b) and 5(c) remain oscillatory, they are no longer periodic due to a linear trend associated with the evolution bands bottoms positions. The relation $\tan \beta_n = (2n - 1) \tan \alpha$ gives slopes β_n of the corresponding envelope straight lines to dependencies of the energies of the bands bottoms on the magnetic field according to (9). Particularly, the slopes in Figure 5(b) are $\tan \beta_1 = 0.1$, $\tan \beta_2 = 0.3$, and $\tan \beta_1 = 0.2$, $\tan \beta_2 = 0.6$ in Figure 5(c) in an excellent accordance with this relation.

The gradual growth of the degree of the quasi-degeneration of the states close to the envelope straight lines, under increasing magnetic field, manifested in Figure 5, could originate a singularity in the density of states. In Figure 6, we display the curves of the density of states of one-electron conical nanotubes with the base radius $R_b = 6a_0^*$, the height $H = 20a_0^*$ calculated for three different top radii $R_t = 1a_0^*, 2a_0^*, 4a_0^*$ and for six different values of the magnetic field. Two dotted straight lines mark the evolution of the singularity peaks positions under increasing magnetic field for states with axial quantum numbers $n = 1$ and $n = 2$, respectively. One can observe a consistent growth of the intensity of peaks related to the increase of the degree of the quasi-degeneration of the corresponding states. The splitting between peaks positions $\Delta = 2\gamma \tan \alpha$, given by relation (9), increases linearly with the growth of the magnetic field, and it depends also on the cone's aperture angle. The larger the aperture angle, the stronger the splitting.

This remarkable alteration of spectral properties of conical nanotubes with a variation of the aperture angle provides

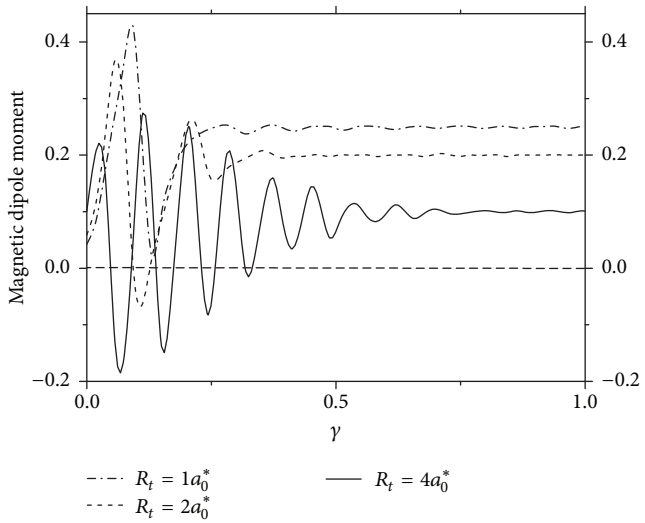

Figure 7: Magnetic dipole momenta of the ground state as functions of the external magnetic field for nanotubes $R_b = 6a_0^*$, $H = 20a_0^*$, and $w = 0.2a_0^*$ and for three different top radii R_t.

also a significant change of magnetic properties of the structure, particularly in the nonlinear dependence of the magnetic dipole moment of the ground state on the magnetic field. The expression for the absolute value of the magnetic dipole moment can be derived using the Hellmann-Feynman theorem.

$$M = \frac{dE_0(\gamma)}{d\gamma}, \tag{10}$$

where $E_0(\gamma)$ is the ground state energy. As it can be seen from right side of Figure 5 the ground state energy in a cylindrical nanotube is a periodic function of the magnetic field. Therefore, the magnetic dipole moment dependence on the magnetic field should be also a periodic function.

As the cylindrical nanotube is transformed in a conical one, the aperture angle is increased, the separation between minima points is consistently reduced, and the amplitude of the ground state energy oscillation is decreased, as it can be seen from curves presented in Figure 5. Therefore, the ground state energy dependence becomes almost linear in accordance with formula (9) for $n = 0$, resulting in the magnetic dipole moment of a conical nanotube almost independent on the magnetic field and equal to the tangent of the aperture angle.

In Figure 7 we show results of calculation of the magnetic dipole moment in conical nanotubes with top radii $R_t = 1a_0^*$, $2a_0^*$ and $4a_0^*$, for which $\tan\alpha$ are equal to 0.25, 0.2, and 0.1, respectively, which are in excellent accordance with our theoretical analysis. Strong dependence of the magnetic moment curves on the aperture angle is seen; their shapes are changed from one, typical for weakly damped AB oscillations, when the aperture angle is small (solid line in Figure 7), up to other, typical for an overdamped oscillator, when the aperture angle becomes large (dash lines). The final part of the curves in all cases presents a horizontal line in which the value of the magnetic dipole moment is independent on the field. According to relation (9) and (10), it is equal to $M = dE_{0,0}(\gamma)/d\gamma = \tan\alpha = 0.1$. This result establishes a direct relation between magnetic properties of the conical nanotube and its morphology.

4. Effect of the Electric Field

Previous results make evident the fact that the hidden symmetry, induced by the increasing magnetic field in systems with the cone-type morphology, provides a quenching of the AB oscillations of the lower energy levels and a multifold quasi-degeneration of the ground state. One can expect that it is possible to suppress or strengthen the escalation of rotational trajectories induced by the magnetic field, by applying a sufficiently strong electric field along the z-axis and breaking in this way the hidden conical symmetry and restoring the AB oscillations. In Figure 8, we show the dependencies of positions of minima $z_{\min}$ of the adiabatic potentials, on the magnetic field, for three different values of the external electric field F applied along the z-axis, given by the relation (9). It is seen that the escalation of the electron circular paths around the axis from the bottom toward the top under increasing magnetic field can be both reinforced in the case of the negative electric field and suppressed in the presence of the positive electric field.

As example, in Figure 8 we point out the positions of potential minima (marked by square solid symbols) of states which are climbing between the bottom and the top of nanotube, for $\gamma = 0.4$. One can see that the positive electric field $F = +0.5$ kV/cm accelerates the escalation toward the cone's top of only states with higher angular momenta $m = 6, 7, 8, 9$. In contrast, the negative electric field $F = -0.5$ kV/cm allows besides the escalation of lower states with $m = 2, 3, 4, 5$. Moreover, in contrast to the first case, in which potentials minima of all four states are equal to zero, in the second all minima are negative being the lowest level located close to the top, while in the last case the lowest level is situated near the bottom.

In Figure 9 we show the lowest energies as functions of the magnetic field and in the presence of the negative $F = -0.5$ kV/cm and positive $F = +0.5$ kV/cm electric fields in one-electron conical nanotube with dimensions $R_b = 6a_0^*$, $R_t = 4a_0^*$, $H = 20a_0^*$, and $w = 0.2a_0^*$. Comparing the curves from Figure 9 with those in Figure 5(c) for zero-electric-field case one can observe that in the presence of the external electric field, independently on its direction, amplitudes of the ground state energy oscillation grow in both cases, but periods of the oscillation, $\Delta\gamma$ for positive and negative electric fields, become essentially different.

In the case of the negative electric field $\Delta\gamma$ in Figure 9(a) is approximately equal to 0.07, which slightly exceeds the value $2/R_b^2$, while the period $\Delta\gamma$ in the presence of the positive electric field in Figure 9(b) is about 0.12, which is in excellent accordance with the value $2/R_t^2$. Thus, the external electric field induces splitting of the quasi-degenerate ground state energy level and it constrains spatially the probability distribution in the state with lowest energy close to the conical nanotube top if the electric field is negative and about the bottom in the case of the positive field.

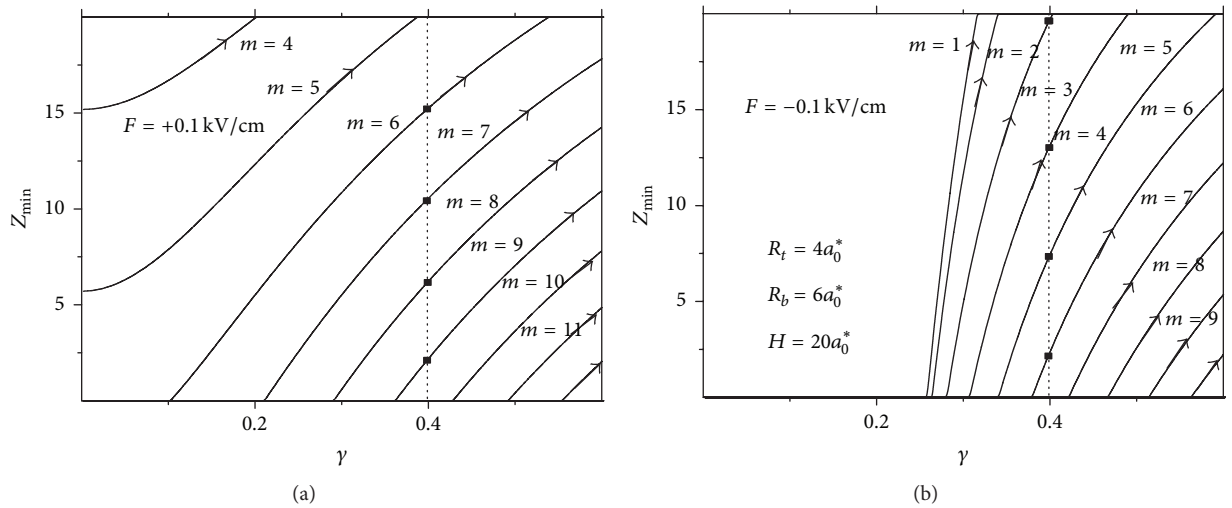

FIGURE 8: Escalation of the minima positions of adiabatic potentials along Z-axis under increasing magnetic field for lower states in conical nanotube with dimensions $R_b = 6a_0^*$, $R_t = 4a_0^*$, $H = 20a_0^*$, and $w = 0.2a_0^*$, for two different values of the electric field.

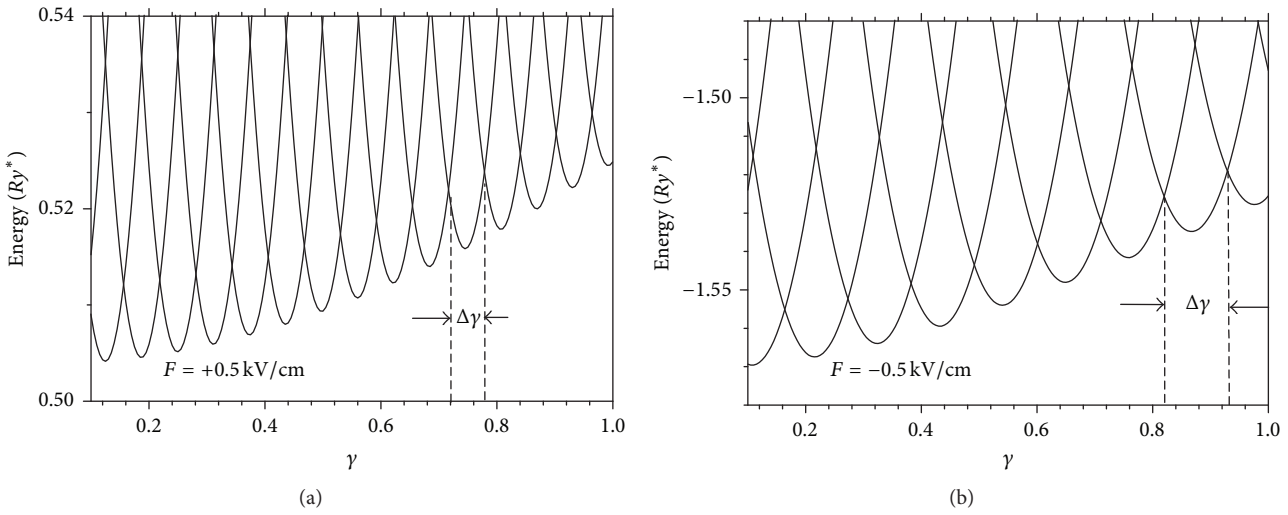

FIGURE 9: The lower energies as functions of the external magnetic field in one-electron conical nanotube with dimensions $R_b = 6a_0^*$, $R_t = 4a_0^*$, $H = 20a_0^*$, and $w = 0.2a_0^*$ in the presence of the electrical fields are (a) $F = -0.5$ kV/cm and (b) $F = +0.5$ kV/cm.

Previous results reveal that the probability density distribution of finding the electron along the z-axis and spectral properties of the one-electron conical nanotube are defined by the interplay between effects of the magnetic and electric fields. The larger the positive electric field is, the bigger the number of the rotational states retained close to the bottom is, and the stronger the magnetic field should be in order to unblock the ascent of rotational states with superior angular momenta. On the contrary, a negative external electric field releases the electron escalation, cooperating in this process with the magnetic field. Therefore, the external electric field essentially affects magnetic properties of this system.

In order to emphasize the effect of the electric field on the magnetic properties of conical nanotube, we present in Figures 10(a) and 10(b) dependencies of the angular and the magnetic momenta on the magnetic field in the presence of the electric field applied along the z-axis at two opposite directions, calculated for the structure with dimensions $R_b = 6a_0^*$, $R_t = 4a_0^*$, $H = 20a_0^*$, and $w = 0.2a_0^*$. One can see that the electric field changes both dependencies in comparison with those presented in Figures 4 and 7 for zero-electric-field case. Particularly, the growth of the angular momentum of the ground state under increasing magnetic field is accelerated in the presence of the negative electric field and it is decelerated when external electric field is positive according to the results presented in Figure 10(a).

The curves of the magnetic dipole moment, shown in Figure 10(b), give an evidence of the AB oscillations similar

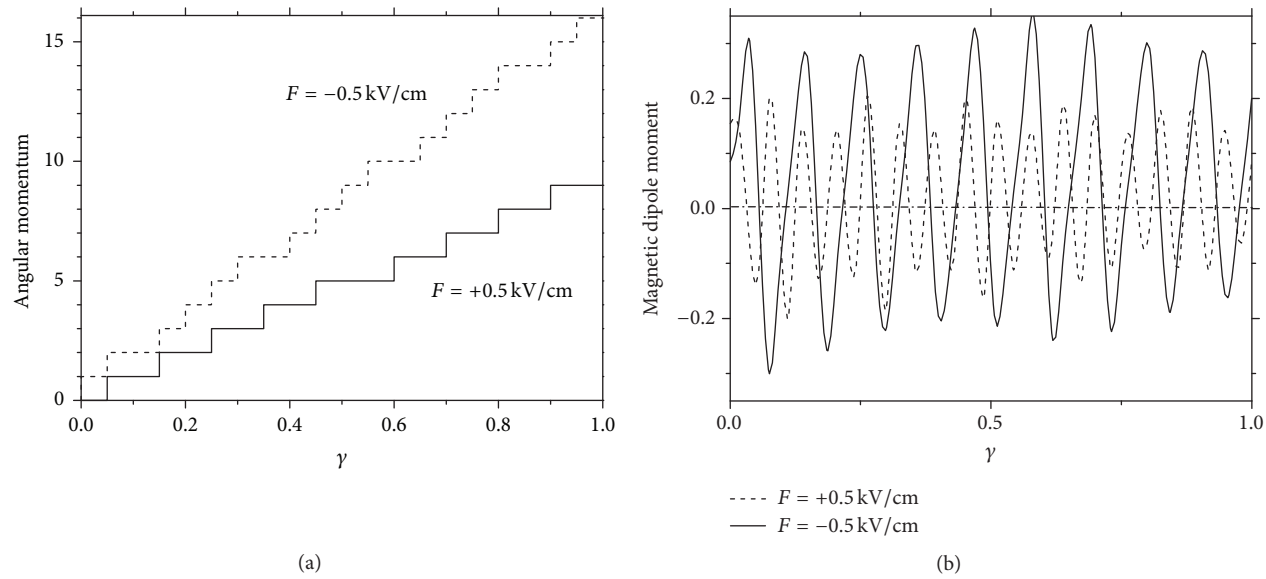

FIGURE 10: Angular (a) and magnetic dipole (b) momenta as functions of the external magnetic field in conical nanotube with $R_b = 6a_0^*$, $R_t = 4a_0^*$, $H = 20a_0^*$, and $w = 0.2a_0^*$ in the presence of the electrical fields $F = -0.5$ kV/cm and $F = +0.5$ kV/cm.

to those in 1D QR with radius $R_t = 6a_0^*$ for $F = +0.5$ kV/cm, while for $F = -0.5$ kV/cm they are similar to those in QR with radius $R_b = 4a_0^*$.

It is seen from Figure 10(b) that the amplitude and the period of the AB oscillation in the case of the negative electric field are two times larger than those in the case of the positive electric field. This result confirms that the electron rotation in the ground state is mainly restrained in a narrow layer close to the cone's top in the first case and close to the bottom at the second case. The special points, where the magnetic dipole moment in Figure 10(b) acquires extreme values, coincide with the crossovers of the energy levels in Figure 9, in which the energy gap between the ground state and the first excited state disappears; that is, the ground state becomes doubly degenerate. This is essentially different from the case of zero-electric-field, in which the ground state is quasi-degenerate with many-fold of levels, almost for all values of the magnetic field, as it can be seen from Figures 4 and 5 and Table 1. Hence, the electric field breaks the conical symmetry of the system, resulting in the splitting of the quasi-degenerate energy levels for all values of the magnetic field except special periodical values for which the ground state is converted to a doubly degenerate.

To clarify how an increasing electric field transforms consistently the nanotube magnetic properties, we display in Figure 11 the curves of the magnetic dipole momenta as functions of the magnetic field for six different values of the positive and negative external electric fields. A consistent evolution of the dependencies with the growth of the electric field is seen; the damping of AB oscillations, significant in the case of the zero-electric-field in Figure 7, is reduced remarkably and it almost disappears when the electric field approaches to 0.5 kV/cm.

5. Summary and Conclusions

In order to analyze the effects of the electric and magnetic fields, applied parallel to symmetry axis, on the spectral and magnetic properties of nanotubes, we consider a simple separable model of a thin axially symmetric one-electron nanotube of conical shape, which offers a comprehensible interpretation of calculation results. We show that the energies and the probability distributions of the electron along the symmetry axis in states with different angular momenta are defined by the interplay between the centrifugal and diamagnetic forces. The centrifugal force pushes the maxima of the electron distributions with different angular momenta toward the cone's bottom, while the diamagnetic force drives them to the cone top. The greater the cone's aperture angle α is, the stronger the competition between these two forces is. As the magnetic field is small, the centrifugal force retains the electron rotation around the axis close to the bottom. This retaining force is proportional to square angular momentum and therefore, when the magnetic field is increased, the peaks of the electron distributions corresponding to different angular momenta begin to climb successively one by one from base toward the top in the order of ascending angular momenta pushed up by the diamagnetic force. We show that such redistribution of the electron's probability density produces a consistent decrease of the amplitude of the AB oscillation of the ground state energy as function of the magnetic field, and when the magnetic field increasing becomes sufficiently large the oscillatory dependence of the ground state energy is quenched and it is transformed into a straight line with the slope exactly equal to the tangent of the aperture angle, while the ground state energy level becomes quasi-degenerate. The number of quasi-degenerate

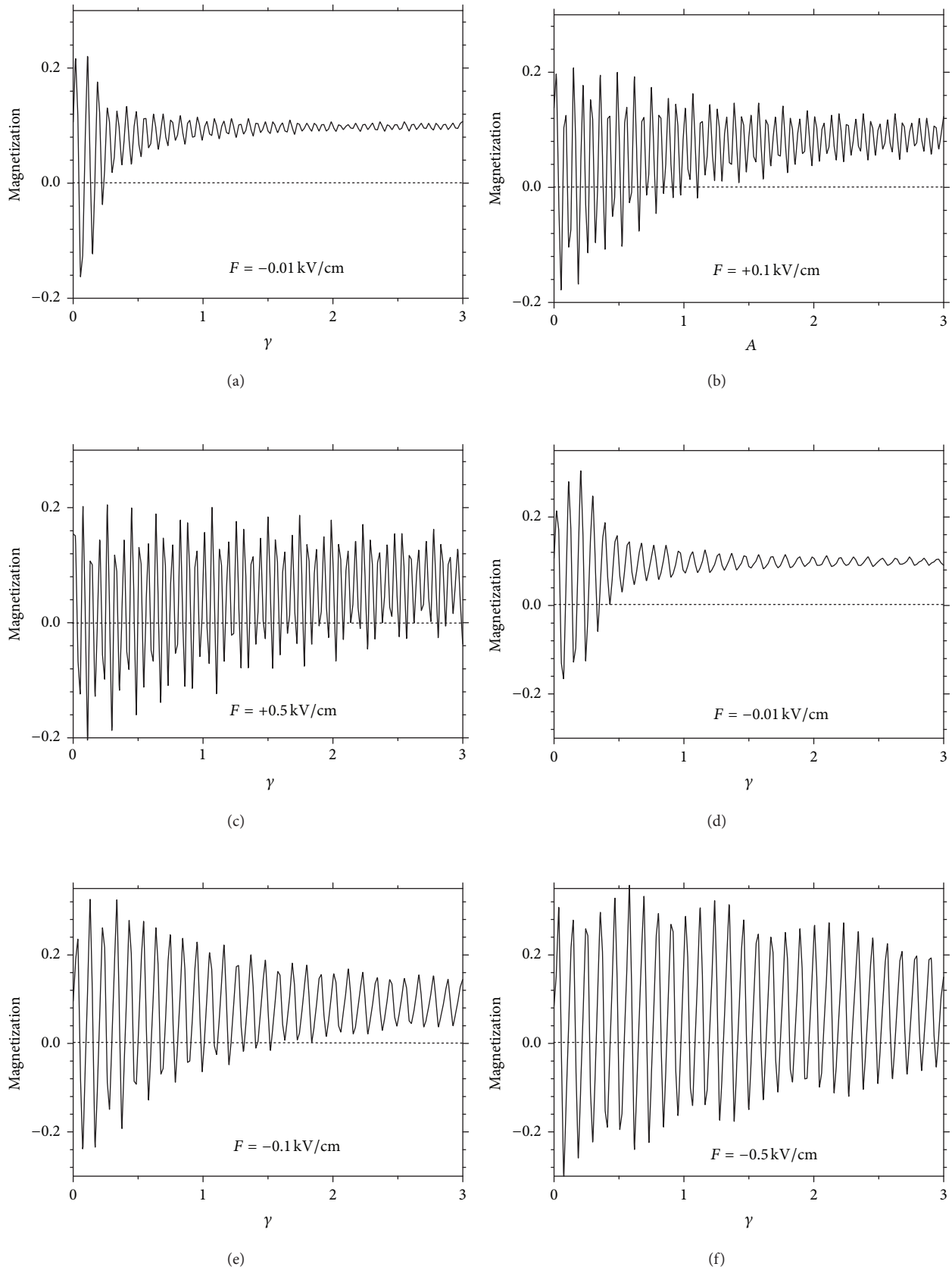

Figure 11: Evolution of the curves of the magnetic dipole moment as functions of the external magnetic field under increasing electrical fields in one-electron conical nanotube with dimensions $R_b = 6a_0^*$, $R_t = 4a_0^*$, $H = 20a_0^*$, and $w = 0.2a_0^*$.

levels rises consistently with the increase of the magnetic field and the aperture angle. We ascribe this effect to a change of the hidden symmetry, induced by the magnetic field in axially symmetric heterostructures, when their morphology is converted from the cylindrical to conical type.

A special form of the dependence of the ground state energy on the magnetic field in the conical nanotube is reflected also on the evolution of the corresponding curves of the density of the states and of the magnetic dipole moment under increasing magnetic field. Particularly, the multiple quasi-degeneration of the levels close to the ground state energy conduces to the appearance of the singularities in the density of states about the bottoms of subbands, corresponding to different axial quantum numbers. We show that the intensity of these peaks and gaps $\Delta = 2\gamma \tan\alpha$ between them grow with the increment of the magnetic field and they depend strongly on the cone's aperture angle. The larger the aperture angle, the higher the peaks and the stronger the splitting.

Similar analysis is presented for one-electron nanotube in the presence of the electric field applied parallel to the cone axis. We show that, by applying a sufficiently strong electric field, it is possible to suppress or reinforce the escalation of rotational trajectories, induced by the magnetic field, breaking in this way the hidden conical symmetry, producing splitting quasi-degenerate levels about the ground state and restoring the AB oscillations.

We show that the positive electric field retains the rotational states close to the bottom increasing the minimum value of the magnetic field required to unblock the ascent of rotational states with superior angular momenta. On the contrary, a negative external electric field releases the electron escalation, cooperating in this process with the magnetic field. Therefore, the external electric field affects essentially the spectral and magnetic properties of this system. Results of calculation of the energies and the magnetic dipole moment approve that the electron rotation in the ground state is mainly restrained in a narrow layer close to the cone's top in the presence of the negative electric field and close to the bottom for the positive electric field. The amplitude of the AB oscillation and the period of the oscillation in the first case are smaller than those in the case of the positive electric field. We ascribe such effect to the possibility of redistribution of electron probability along the axis under external electric field. Our analysis establishes a fascinating possibility to control the magnetic properties of nanotubes by means of an external electric field.

We believe that our analysis reveals a possibility for detection of the coupling between the polarization and magnetization in conically shaped nanostructures, resulting from the quantum-size effect. Similar coupling between magnetic and electric properties of ferroelectric and ferromagnetic materials consisting in the appearance of an electric polarization under the application of a magnetic field or in the appearance of a magnetization under the application of an electric field is called the magnetoelectricity [24, 25]. One can expect that similar effect associated with the quantum confinement might be presented in tubes with nonuniform cross-section profiles. The more abrupt the variation of the cross-sections radii along the axis in such structures is, the stronger the coupling between the polarization and magnetization could be.

Competing Interests

The authors declare that there is no conflict of interests regarding the publication of this paper.

Acknowledgments

This work was financed by the Universidad Industrial de Santander (UIS) through Vicerrectoría de Investigación y Extensión, DIEF de Ciencias (Cod. 5710), and Patrimonio Autónomo del Fondo Nacional para el Financiamiento de la Ciencia en Tecnologías para la Innovación Francisco José de Caldas Contrato RC-no. 275-2011 and the Cod. no. 1102-05-16923 subscribed with Colciencias.

References

[1] Z. L. Wang, "Characterizing the structure and properties of individual wire-like nanoentities," *Advanced Materials*, vol. 12, no. 17, pp. 1295–1298, 2000.

[2] J. Hu, T. W. Odom, and C. M. Lieber, "Chemistry and physics in one dimension: synthesis and properties of nanowires and nanotubes," *Accounts of Chemical Research*, vol. 32, no. 5, pp. 435–445, 1999.

[3] Y. Xia, P. Yang, Y. Sun et al., "One-dimensional nanostructures: synthesis, characterization, and applications," *Advanced Materials*, vol. 15, no. 5, pp. 353–389, 2003.

[4] B. Wang and P. W. Leu, "Enhanced absorption in silicon nanocone arrays for photovoltaics," *Nanotechnology*, vol. 23, no. 19, Article ID 194003, 2012.

[5] B. Wang, E. Stevens, and P. W. Leu, "Strong broadband absorption in GaAs nanocone and nanowire arrays for solar cells," *Optics Express*, vol. 22, supplement 2, pp. A386–A395, 2014.

[6] R. Yu, Q. Lin, S.-F. Leung, and Z. Fan, "Nanomaterials and nanostructures for efficient light absorption and photovoltaics," *Nano Energy*, vol. 1, no. 1, pp. 57–72, 2012.

[7] I. Friedler, C. Sauvan, J. P. Hugonin, P. Lalanne, J. Claudon, and J. M. Gérard, "Solid-state single photon sources: the nanowire antenna," *Optics Express*, vol. 17, no. 4, article 2095, 2009.

[8] S. L. Diedenhofen, O. T. A. Janssen, G. Grzela, E. P. A. M. Bakkers, and J. Gómez Rivas, "Strong geometrical dependence of the absorption of light in arrays of semiconductor nanowires," *ACS Nano*, vol. 5, no. 3, pp. 2316–2323, 2011.

[9] V. M. Fomin, Ed., *Physics of Quantum Rings*, Springer, Berlin, Germany, 2014.

[10] L. Wendler, V. M. Fomin, A. V. Chaplik, and A. O. Govorov, "Optical properties of two interacting electrons in quantum rings: optical absorption and inelastic light scattering," *Physical Review B*, vol. 54, no. 7, pp. 4794–4810, 1996.

[11] A. V. Chaplik, "Retardation effects in plasma oscillations of a bilayer structure," *JETP Letters*, vol. 101, no. 8, pp. 545–548, 2015.

[12] R. A. Römer and M. E. Raikh, "Aharonov-Bohm effect for an exciton," *Physical Review B*, vol. 62, no. 11, pp. 7045–7049, 2000.

[13] F. Ding, N. Akopian, B. Li et al., "Gate controlled Aharonov-Bohm-type oscillations from single neutral excitons in quantum rings," *Physical Review B*, vol. 82, no. 7, Article ID 075309, 2010.

[14] M. D. Teodoro, V. L. Campo, V. Lopez-Richard et al., "Aharonov-bohm interference in neutral excitons: effects of built-in electric fields," *Physical Review Letters*, vol. 104, no. 8, Article ID 086401, 2010.

[15] L. C. Porras and I. D. Mikhailov, "Neutral and positively charged excitons in quantum ring," *Physica E*, vol. 53, pp. 41–47, 2013.

[16] M. Bayer, "Exciton complexes in self-assembled In(Ga)As/GaAs quantum dots," in *Single Quantum Dots: Fundamentals, Applications, and New Concepts*, vol. 90 of *Topics in Applied Physics*, pp. 93–146, Springer, Heidelberg, Germany, 2003.

[17] Y. V. Pershin and C. Piermarocchi, "Laser-controlled local magnetic field with semiconductor quantum rings," *Physical Review B*, vol. 72, no. 24, Article ID 245331, 2005.

[18] A. Bruno-Alfonso and A. Latgé, "Quantum rings of arbitrary shape and non-uniform width in a threading magnetic field," *Physical Review B*, vol. 77, no. 20, Article ID 205303, 2008.

[19] F. Rodríguez-Prada, L. F. García, and I. D. Mikhailov, "One-electron quantum ring of non-uniform thickness in magnetic field," *Physica E*, vol. 56, pp. 393–399, 2014.

[20] W. Gutiérrez, L. F. Garca, and I. D. Mikhailov, "Coupled donors in quantum ring in a threading magnetic field," *Physica E*, vol. 43, no. 1, pp. 559–566, 2010.

[21] K. Tsumura, S. Nomura, P. Mohan, J. Motohisa, and T. Fukui, "Aharonov-Bohm oscillations in photoluminescence from charged exciton in quantum tubes," *Japanese Journal of Applied Physics*, vol. 46, no. 17–19, pp. L440–L443, 2007.

[22] K. Kubota, P. O. Vaccaro, N. Ohtani, Y. Hirose, M. Hosoda, and T. Aida, "Photoluminescence of GaAs/AlGaAs micro-tubes containing uniaxially strained quantum wells," *Physica E*, vol. 13, no. 2–4, pp. 313–316, 2002.

[23] F. J. Betancur, I. D. Mikhailov, and L. E. Oliveira, "Shallow donor states in GaAs-(Ga, Al)As quantum dots with different potential shapes," *Journal of Physics D: Applied Physics*, vol. 31, no. 23, pp. 3391–3396, 1998.

[24] J. Zhai, J. Li, D. Viehland, and M. I. Bichurin, "Large magnetoelectric susceptibility: the fundamental property of piezoelectric and magnetostrictive laminated composites," *Journal of Applied Physics*, vol. 101, Article ID 014102, 2007.

[25] J. P. Rivera, "A short review of the magnetoelectric effect and related experimental techniques on single phase (multi-) ferroics," *The European Physical Journal B*, vol. 71, no. 3, pp. 299–313, 2009.